MARMARA
MEDICAL JOURNAL

Original Article

https://dergipark.org.tr/tr/pub/marumj

NADPH oxidase-2 inhibitor apocynin attenuates high-fat diet-induced kidney and bladder injury

Fatma KANPALTA MUSTAFAOGLU[1], Busra ERTAS[2], Goksel SENER[3], Feriha ERCAN[1]

[1] Department of Histology and Embryology, School of Medicine, Marmara University, Istanbul, Turkiye
[2] Department of Pharmacology, School of Pharmacy, Marmara University, Istanbul, Turkey
[3] Department of Pharmacology, School of Pharmacy, Fenerbahce University, Istanbul, Turkiye
Corresponding Author: Feriha ERCAN
E-mail: fercan@marmara.edu.tr

Submitted: 08.08.2024 **Accepted:** 07.02.2025

ABSTRACT

Objective: This study aimed to evaluate the effects of NADPH oxidase-2 (NOX-2) inhibitor apocynin (APC) on high-fat diet (HFD)-induced renal and bladder injury.

Materials and Methods: Wistar albino rats were divided into 4 groups: Control, HFD, HFD+dimetyl sulfoxide (DMSO), and HFD+APC. Rats in HFD, HFD+DMSO, and HFD+APC groups were fed with HFD for sixteen weeks. In the last 4 weeks of the experiment, either DMSO or APC (25 mg/kg, dissolved in DMSO) was applied to the HFD+DMSO or HFD+APC groups. Lipid profiles and leptin values were measured in blood serum. Renal and bladder oxidant/antioxidant parameters, histological changes in the tissues, NOX-2-, nuclear factor kappa B (NF-κB)-immunopositive and apoptotic cells were evaluated.

Results: At the end of the experiment, leptin, cholesterol, and triglyceride levels were higher and high-density lipoprotein levels were lower in the HFD and HFD+DMSO groups compared to controls. In these experimental groups, an increase in malondialdehyde, 8-hydroxy-deoxyguanosine and myeloperoxidase levels and a decrease in glutathione levels, as well as an increase in collagen, NOX-2 – and NFκ-B-immunopositive and apoptotic cells were found. Also, a deterioration in kidney and bladder morphology was observed. All these biochemical and histopathological findings improved in the HFD+APC group.

Conclusion: High-fed diet causes renal and bladder injury by increasing NOX-2 activity and inflammation via oxidative stress. APC might alleviate tissue injury by inhibiting oxidative stress.

Keywords: Apocynin, Bladder, High-fat diet, Kidney, Oxidative stress

1. INTRODUCTION

Obesity, an increasing health problem over the last thirty years, is defined by excessive fat accumulation in adipose and nonadipose tissues [1]. Common causes of obesity are insufficient physical activity and energy-dense foods [2, 3]. High-fat diet (HFD)-induced obesity is related to many metabolic diseases, chronic kidney disease (CKD), and bladder obstruction [3, 4]. Moreover, obesity has been shown to damage the kidneys even without hypertension or diabetes [1, 5].

Obesity-induced kidney and bladder injury mechanisms are unclear, but increased circulating fatty acids [6] and leptin-induced excessive formation of reactive oxygen species (ROS) directly damage the morphology and function of the urinary system [7]. NADPH oxidase (NOX) is a multicomponent transmembrane enzyme family with 7 isoforms, NOX-1-5 and DUOX1-2, that generate ROS [8]. NOX-2 activation is involved in pathologies of the kidney [7] and bladder [9], inducing the inflammatory response [10] and fibrosis [11].

Apocynin (APC), which acts as a NOX-2 inhibitor [12], has been shown to attenuate bladder damage caused by arsenite [9], ischemia/reperfusion-induced testicular injury [13], HFD-induced testis injury [14] and suppresses leptin from adipose tissue in HFD-induced obesity [10]. Therefore, the present study goaled to study the effects of APC on HFD-induced renal and urinary bladder damage by histological and biochemical methods.

How to cite this article: Kanpalta Mustafaoglu F, Ertas B, Sener G, Ercan F. NADPH oxidase-2 inhibitor apocynin attenuates high-fat diet-induced kidney and bladder injury. Marmara Med J 2025;38 (2): 171-178. doi: 10.5472/marumj.1706664

ISSN: 1309-9469

http://doi.org/10.5472/marumj.1706664
Marmara Med J 2025;38(2): 171-178

2. MATERIALS and METHODS

Animals and experimental design

Wistar albino rats (male, 8-week-old, 200-250 g) were obtained from the Marmara University Experimental Animals Research and Implementation Centre. They were kept under a standard laboratory environment (12-h light/dark cycle, 50-60% relative moisture, and 23-25°C heat) with ad libitum reach to water and chow. This study was endorsed by Marmara University, Animal Care and Use Ethical Committee for Experimental Animals (date: 10.02.2020, approval number: 09.2020.mar).

The rats (n=32) were randomly divided into 4 equal groups and fed with a standard diet (8% fat, 24% protein, 68% carbohydrate,) or HFD (45% fat, 20% protein, 35% carbohydrate,) for 16 weeks. In the last 4 weeks, either dimethyl sulfoxide (DMSO) or 25 mg/kg APC dissolved in 15% DMSO (5 days a week) was administered to the HFD+DMSO or HFD+APC groups respectively by orogastric gavage [13]. The body weight of the rats was measured weekly throughout the experiment. At the end of the study, rats were decapitated and blood, kidney, and bladder samples were collected.

Measuring serum high-density lipoprotein, total cholesterol, triglyceride, and leptin levels

Serum high-density lipoprotein (HDL), total cholesterol, triglyceride, and leptin levels were measured using ELISA kits (Elabscience Biotechnology, USA) according to the manufacturer's directives.

Measuring tissue malondialdehyde, glutathione, 8-hydroxy-deoxyguanosine, and myeloperoxidase levels

The malondialdehyde (MDA) and 8-hydroxy-deoxyguanosine (8-OHdG) levels for oxidative stress, glutathione (GSH) levels for antioxidant activity, and myeloperoxidase (MPO) activity for inflammation were measured in renal and bladder homogenates using ELISA kits (MyBiosource, Inc., San Diego, USA) according to the manufacturer's directives.

Histological preparation and histopathological scoring

Kidney and bladder samples were fixed in 10% formalin and processed for paraffin embedding. Five – µm-thick paraffin sections were stained with hematoxylin and eosin (H&E) for morphological evaluation and stained with Sirius red for evaluation of collagen distribution and acidified toluidine blue (pH: 2-3) for evaluation of mast cells.

In the H&E stained sections, 5 random areas that did not coincide were examined, and a semiquantitative histopathological score was given (severe damage: 3; moderate damage: 2; mild damage: 1; no damage: 0). Kidney samples were evaluated for enlargement of Bowman's space, glomerular congestion, cell debris in the tubular lumen, and tubular damage [15]. Bladder sections were evaluated for urothelial damage, mucosal inflammatory cell infiltration, and mucosal and muscular inflammatory cell infiltration [16]. The highest histopathological damage score was determined to be 9 for each tissue. Sirius red-stained kidney and bladder sections were measured as a percentage of areas by using Image J Software. Mast cell counts were performed in five non-overlapping fields on toluidine blue stained bladder sections under the 40x objective of the light microscope.

Immunohistochemical Methods

NOX-2, nuclear factor kappa B (NF-κB), and transforming growth factor (TGF)-β1 immunohistochemistry procedures were applied to the deparaffinized and rehydrated sections. They were incubated in 3% H_2O_2 solution, boiled in citrate buffer solution for antigen recovery, washed with phosphate-buffered saline (PBS), and dripped with blocking solution (Abcam, Cambridge, UK). NOX-2 (1:200; Bioss, Massachusetts, USA) and NF-κB (1:1000; Cell Signalling Technology, Massachusetts, USA) primary antibodies were applied to both kidney and bladder sections, and TGF-β1 primary antibody (1:200; Santa Cruz, Texas, USA) was applied only to kidney sections at 4°C overnight. After washing with PBS, sections were placed in a biotinylated secondary antibody (UltraTek Hrp Anti-Polyvalent, ScyTek, Utah, USA). After washing with PBS, the sections were placed in streptavidin peroxidase and then washed with PBS. 3,3-diaminobenzidine tetrahydrochloride (DAB) was applied and counterstained with hematoxylin. Five similar areas from each NOX-2-, NF-κB-, and TGF-β1-stained sections were evaluated. The percentage of immunoreactivity (IR) was estimated by using the Image J Software program.

Terminal deoxynucleotidyl transferase-mediated dUTP nick-end labeling method

The terminal deoxynucleotidyl transferase-mediated dUTP nick-end labeling (TUNEL) technique was performed in the renal and bladder tissues according to a kit (Apoptag Plus, In Situ Apoptosis Detection Kit, Millipore, Darmstadt, Germany). TUNEL-positive cells were counted in five similar areas in each section under the 40x objective of the light microscope.

All stained sections were evaluated under a photomicroscope (Olympus BX51, Tokyo Japan). The experimental design and evaluated biochemical and histological parameters were summarized in Figure 1.

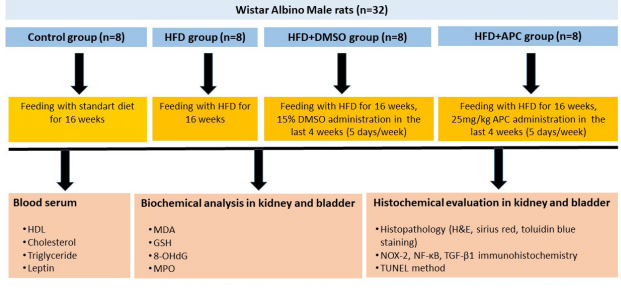

Figure 1. *Experimental design, lipid profile and leptin analysis in blood serum, biochemical and histological analysis parameters in kidney and bladder samples.*

http://doi.org/10.5472/marumj.1706664
Marmara Med J 2025;38(2): 171-178

Statistical analysis

Histological and biochemical data were analyzed by using an instant statistical analysis package (Prism 8.0 GraphPad Software, San Diego, CA, USA). The statistical analysis was performed using one-way or two-way ANOVA and Tukey's multiple comparison tests. The data were given as mean ± standard error of the mean (SEM). A p value <0.05 was accepted as significant.

3. RESULTS

Body weight change

The body weights of rats in the HFD, HFD+DMSO, and HFD+APC (p<0.01-p<0.001) groups increased significantly compared to the control group at the end of the experiment (Figure 2).

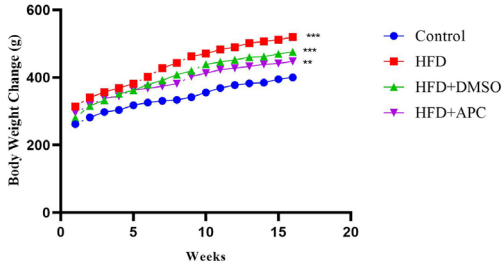

Figure 2: *Body weight changes in the experimental groups. ** p<0.01 and *** p<0.001 versus control group.*

Serum HDL, total cholesterol, triglyceride and leptin levels

HDL level was lower and total cholesterol, triglyceride, and leptin levels were higher in the HFD and HFD+DMSO groups compared to the control group (p<0.001) at the end of the study. These values were alleviated in the HFD+APC group compared to the HFD and HFD+DMSO groups (p<0.001; Figure 3).

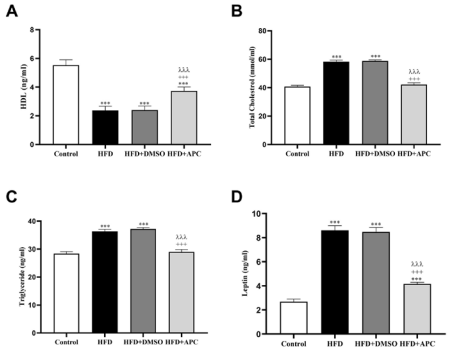

Figure 3: *Serum HDL (A), total cholesterol (B), triglyceride (C) and leptin (D) levels are seen in the experimental groups. *** p<0.001 versus control group, +++ p<0.001 versus HFD group, λλλ p<0.001 versus HFD+DMSO group.*

Tissue MDA, GSH, 8-OHdG, and MPO levels

In renal samples, MDA, 8-OHdG, and MPO levels were higher and GSH levels were lower in the HFD and HFD+DMSO groups compared to the control group (p<0.01 – p<0.001). MDA, 8-OHdG, and MPO levels were higher in the HFD+APC group compared to the control group (p<0.05 – p<0.001). But, MDA, 8-OHdG, and MPO levels (p<0.05-p<0.001) were lower and GSH levels (p<0.05) were higher in the HFD+APC group compared to the HFD and HFD+DMSO groups (Figure 4A-D).

In bladder samples, MDA, 8-OHdG, and MPO levels were higher and GSH levels were lower in the HFD and HFD+DMSO groups compared to the control group (p<0.001). MDA and 8-OHdG levels were higher and GSH levels were lower in the HFD+APC group than in the control group (p<0.05-p<0.01). However, MDA and MPO levels were lower and GSH level was higher in the HFD+APC group compared to the HFD and HFD+DMSO groups (p<0.05-p<0.001; Figure 4E-H).

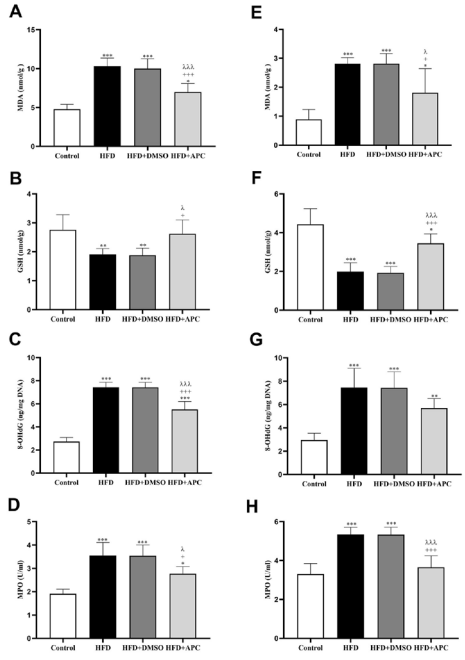

Figure 4: *MDA (A, E), GSH (B, F), 8-OHdG (C, G), and MPO (D, H) levels in renal (A-D) and bladder (E-H) samples are seen in the experimental groups. * p<0.05, ** p<0.01 and *** p<0.001 versus control group; + p<0.05 and +++ p<0.001 versus HFD group; λ p<0.05 and λλλ p<0.001 versus HFD+DMSO group.*

Histopathological findings

Regular kidney morphology was seen in the control group. Dilatated Bowman's space, mild glomerular and interstitial vascular congestion, degenerated tubules, and inflammatory cell infiltration were seen in the HFD and HFD+DMSO groups. However, these histopathological findings were ameliorated in the HFD+APC group (Figure $5A_1$-D_1). The histopathological

http://doi.org/10.5472/marumj.1706664
Marmara Med J 2025;38(2): 171-178

score was higher in both the HFD and HFD+DMSO groups than that of the control group (p<0.001). APC treatment lowered this score compared to the HFD and HFD+DMSO groups (p<0.05; Figure 5E$_1$). Normal collagen distribution was observed in the control group. However, an increase in collagen distribution was observed around the renal corpuscles and tubules in the HFD and HFD+DMSO groups. Collagen distribution was quite regular in the HFD+APC group (Figure 5A$_2$-D$_2$). The percentage of collagen deposition was higher in both the HFD (p<0.001) and HFD+DMSO (p<0.01) groups than that of the control group. This value was lower in the HFD+APC group than in the HFD (p<0.01) and HFD+DMSO (p<0.05) groups (Figure 5E$_2$).

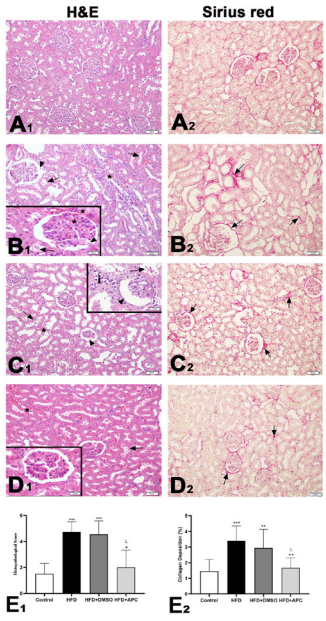

Figure 5: *Representative light micrographs of H&E (A1-D1) and Sirius red (A2-D2) stained kidney samples, the histopathological score (E1) and percentage of collagen amount (E2) are seen in the control (A1, A2), HFD (B1, B2), HFD+DMSO (C1, C2) and HFD+APC (D1, D2) groups. B1-D1: Arrow: damaged tubules with debris in the lumen; *: vascular congestion in glomeruli and interstitium; arrowhead: cellular debris in glomeruli (insert B1) and fibrotic glomeruli (insert C1); i: inflammatory cell infiltration in the interstitium. B2-D2: Arrow: collagen distribution. ** p<0.01 and *** p<0.001 versus control group; + p<0.05 and ++ p<0.01 versus HFD group; λ p<0.05 versus HFD+DMSO group.*

Regular bladder morphology was observed in the standard diet-fed rats. Mild urothelial damage, moderate vascular congestion in the lamina propria, and inflammatory cell infiltration were seen in the HFD and HFD+DMSO groups. Quite normal morphology was observed despite local urothelial damage in the HFD+APC group (Figure 6A$_1$-D$_1$). The histopathological score was higher in both the HFD and HFD+DMSO groups than the control group (p<0.001). APC treatment lowered this score compared to the HFD and HFD+DMSO groups (p<0.01; Figure 6E$_1$). Regular distribution of the collagen fibers in bladder samples was observed in the control group. Disrupted muscle fiber organization and an increase in collagen fibers in the muscle layer were seen in the HFD and HFD+DMSO groups. Quite a regular collagen distribution was found in the HFD+APC group (Figure 6A$_2$-D$_2$). The percentage of collagen amount in the muscle layer was higher in both the HFD (p<0.001) and HFD+DMSO (p<0.01) groups when compared to the control group. The percentage of collagen amount was lower in the HFD+APC group than in the HFD (p<0.01) and HFD+DMSO (p<0.05) groups (Figure 6E$_2$). A few numbers of granulated mast cells were seen in the lamina propria of the control group. Migration of mast cells to the urothelium and increase of mast cells in the lamina propria and muscle layer were found in the HFD and HFD+DMSO groups. However, a decrease in the number of mast cells was observed in the lamina propria and muscle layer of the HFD+APC group (Figure 6A$_3$-D$_3$). The total number of mast cells per area was higher in both the HFD (p<0.05) and HFD+DMSO (p<0.01) groups compared to the control group. A decrease of mast cells was observed in the HFD+APC group compared to the HFD (p<0.05) and HFD+DMSO (p<0.01) groups (Figure 6E$_3$).

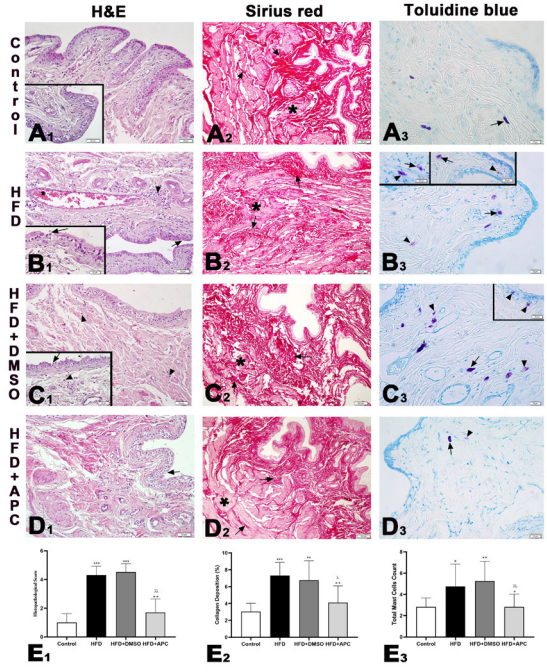

Figure 6: *Representative light micrographs of H&E (A1-D1), Sirius red (A2-D2), and toluidine blue (A3-D3) stained bladder samples, histopathological score (E1), percentage of collagen deposition (E2) and total mast cell count (E3) are seen in the control (A1-A3), HFD (B1-B3), HFD+DMSO (C1-C3) and HFD+APC (D1-D3) groups. B1-D1: Arrow: mild epithelial damage; *: vascular congestion; arrowhead: inflammatory cell infiltration. A2-D2: *: muscle bundles; arrow: collagen distribution. A3-D3: Arrow: granulated mast cells; arrowhead: degranulated mast cells. * p<0.05, ** p<0.01 and *** p<0.001 versus control group; + p<0.05 and ++ p<0.01 versus HFD group; λ p<0.05 and λλ p<0.01 versus HFD+DMSO group.*

http://doi.org/10.5472/marumj.1706664
Marmara Med J 2025;38(2): 171-178

NOX-2, NF-κB and TGF-β1 immunohistochemistry findings

In kidney samples, a few NOX-2 – and NF-κB-immunopositive tubular epithelial cells and glomerular cells, and some TGF-β1 mesangial and interstitial-immunopositive cells were found in the control group. An increase of NOX-2-, NF-κB-, and TGF-β1-immunopositive cells was found in both the HFD and HFD+DMSO groups. The number of NOX-2-, NF-κB, and TGF-β1-immunopositive cells decreased in the HFD+APC group compared to the HFD and HFD+DMSO groups. The percentage of NOX-2 IR ($p<0.05$), NF-κB IR ($p<0.001$), and TGF-β1 IR areas was higher in the HFD group than in the control group. But, the percentage of NOX-2 IR ($p<0.01$), NF-κB IR ($p<0.01$), and TGF-β1 IR areas ($p<0.05$) was lower in the HFD+APC group than in the HFD group (Figure 7A_1-E_3).

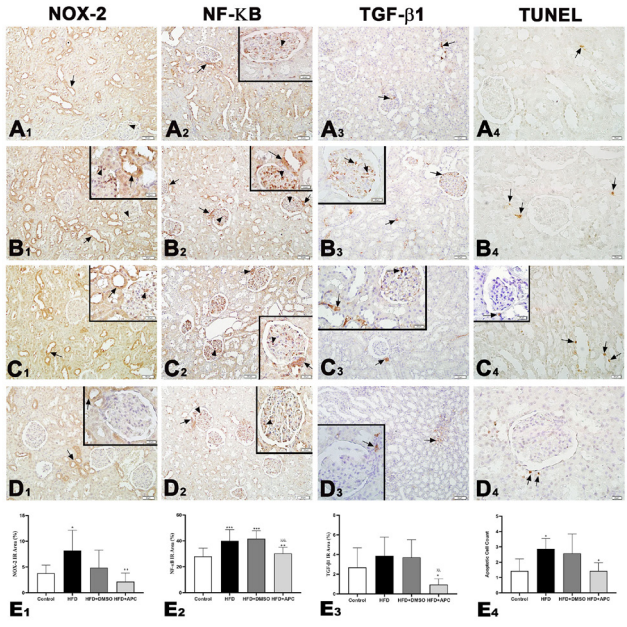

Figure 7: *Representative light micrographs of NOX-2 (A1-D1), NF-κB (A2-D2), TGF-β1 (A3-D3) immunostained and TUNEL (A4-D4) stained kidney samples, and NOX-2 (E1), NF-κB (E2) and TGF-β1 (E3) IR areas and apoptotic cell counts (E4) are seen in the control (A1-A4), HFD (B1-B4), HFD+DMSO (C1-C4) and HFD+APC (D1-D4) groups. NOX-2 – and NF-κB-immunopositive tubular epithelial cells (arrow) and glomerular mesangial cells (arrowhead), TGF-β1-immunopositive cells (arrow) and TUNEL-positive cells (arrow) are seen in the experimental groups. * $p<0.05$ and *** $p<0.001$ versus control group; + $p<0.05$ and ++ $p<0.01$ versus HFD group; λλ $p<0.01$ and λλλ $p<0.001$ versus HFD+DMSO group.*

In bladder samples, a few numbers of NOX-2 and NF-κB immunopositive cells in the urothelium and muscular layer were observed in the control group. Increased NOX-2 – and NF-κB-immunopositive urothelial and inflammatory cells were found in both the HFD and HFD+DMSO groups. The number of NOX-2 – and NF-κB-immunopositive cells was reduced in the HFD+APC group compared to the HFD group. The percentage of NOX-2 and NF-κB IR areas was higher in the HFD group compared to the control group ($p<0.05$). However, the percentage of NOX-2 ($p<0.05$) and NF-κB ($p<0.001$) IR areas was lower in the HFD+APC group than in the HFD group (Figure 8A_1-E_2).

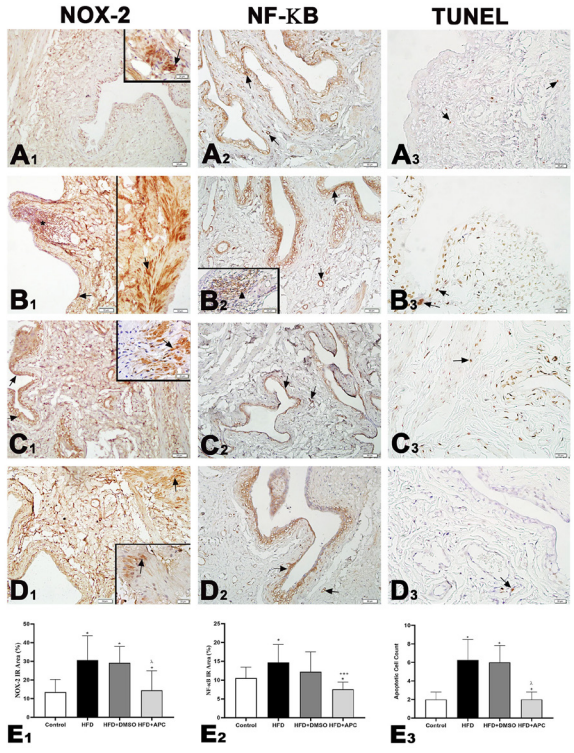

Figure 8: *Representative light micrographs of NOX-2 (A1-D1) and NF-κB (A2-D2), immunostained, and TUNEL (A3-D3) stained bladder samples and NOX-2 (E1) and NF-κB IR (E2) areas and apoptotic cell counts (E3) are seen in the control (A1-A3), HFD (B1-B3), HFD+DMSO (C1-C3) and HFD+APC (D1-D3) groups. NOX-2-immunopositive urothelial (arrow), inflammatory (*) and smooth muscle cells (arrows: inserts A1-D1); NF-κB-immunopositive (arrow), inflammatory (arrowhead: insert B2) and TUNEL-positive (arrow) cells are seen in the experimental groups. * $p<0.05$ versus control group; + $p<0.05$ and +++ $p<0.001$ versus HFD group; λ $p<0.05$ versus HFD+DMSO group.*

TUNEL findings

In both kidney and bladder samples, the TUNEL-positive cells were higher in the HFD group ($p<0.05$) than in the standard diet fed-control group. However, TUNEL-positive cells were lower in the HFD+APC group ($p<0.05$) than in the HFD group in both kidney (Figure 7A_4-E_4) and bladder samples (Figure 8A_3-E_3).

4. DISCUSSION

Obesity has been shown to be the underlying cause of many problems, such as cardiovascular diseases, CKD, and bladder dysfunction [1, 2, 6]. Obesity can result from a sedentary

http://doi.org/10.5472/marumj.1706664
Marmara Med J 2025;38(2): 171-178

lifestyle and high carbohydrate, protein, or fat diets [2-4]. In many studies, HFD feeding causes weight gain in experimental animals [2, 3, 14, 17]. In this study, we found that the body weight of rats increased in the HFD, HFD+DMSO, and HFD+APC groups compared to the control group. APC treatment of HFD-fed C57BL/6 mice decreased leptin and insulin resistance, thus contributing to weight reduction [10]. However, in our study, serum leptin levels decreased with APC treatment, no weight reduction was observed. This may be due to the difference in experimental animal species or the duration of treatment.

Obesity is characterized by increased free fatty acids [2, 14, 18] in the blood and the associated accumulation of white adipose tissue [1]. When the capacity of adipocytes is exceeded, ectopic accumulation is observed in peripheral tissues [4, 19]. Researches have shown that obese animals have an increase in blood glucose [4, 6], serum triglyceride and cholesterol levels, and a decrease in HDL levels [2, 4, 14, 18]. It was shown that HFD feeding caused an increase in serum lipids, resulting in severe lipid accumulation in the kidney, glomerulomegaly, and dilated tubule damage [4]. In addition to lipid toxicity, hyperleptinemia has also been observed in obesity [1]. Leptin, one of the adipokines released by hypertrophic fat tissue [10], not only controls appetite through the central nervous system but also activates NF-κB via a paracrine effect in peripheral tissues where its receptor is located in peripheral tissue [20]. High serum leptin levels caused increased inflammation in both renal tubule epithelial and mesangial cells, while leptin and NOX-2 knockout mice had no inflammation in these cells despite high serum cholesterol and triglyceride levels [7]. In this study, serum HDL levels decreased in the HFD and HFD+DMSO groups as a result of HFD feeding. Triglyceride, total cholesterol, and leptin levels increased, as did histological tissue damage and NOX-2-immunopositive cells in the renal and bladder samples. The APC treatment showed an antioxidant effect by inhibiting NOX-2 and resulted in histological improvement in the kidney and bladder by bringing serum leptin and lipid profiles to the level of the control group.

Free fatty acids are important substances that cause oxidative stress. Antioxidant compounds provide stability against ROS damage. In a previous study, obesity was shown to decrease serum antioxidant levels, increase serum leptin levels, and result in podocyte and tubular epithelial damage, inflammatory cell infiltration, interstitial congestion, and fibrosis [1]. HFD-induced obesity leads to lipid peroxidation due to an increase in ROS, an increase in MDA, which is a lipid peroxidation product, and a decrease, in the level of GSH, an antioxidant compound in both kidney and bladder samples [21]. In ischemia–reperfusion-induced testicular damage, 20 and 40 mg/kg doses of APC treatment have been shown to decrease MDA levels and increase GSH levels [13]. Moreover, it has been shown that APC treatment ameliorated HFD-induced testis damage [14] and monosodium glutamate-induced kidney damage [22] with a reduction in MDA and an increase in GSH levels. In our study, increased MDA levels and decreased GSH levels were found in renal and bladder samples of the HFD and HFD+DMSO groups. On the other hand, it was observed that these two parameters were reduced in the HFD+APC group in comparison with the HFD group.

It was reported that ROS targets DNA to stabilize itself. Faulty DNA replication has been shown to cause mutation, cell apoptosis, or cancer formation [9]. The 8-OHdG is one of the most common markers of oxidative damage of DNA [23]. In the study of diabetic nephropathy induced by HFD and streptozotocin, increased MDA, 8-OHdG, caspase-3 and apoptotic cell numbers have been shown to be due to oxidative damage and apoptosis in kidney tissue [24]. Increased urothelial apoptosis in bladder biopsies from patients with CKD has been thought to be associated with barrier defects [25]. It has been shown that arsenic-induced NOX-mediated ROS production causes bladder epithelial hyperplasia and an increase in 8-OHdG, while APC treatment prevents apoptosis without affecting regenerative proliferation [9]. Similar to the previous studies, the tissue 8-OHdG level and TUNEL-positive cell count increased in the renal and bladder tissues of HFD groups in the present study. APC treatment decreased these parameters by inhibiting oxidative stress in the kidney and bladder.

The persistence of ROS has been shown to activate inflammation and exacerbate organ damage. In a study on obesity, it was shown that an increase in monocyte chemoattractant protein-1, interleukin-6 (IL-6), and leptin levels in fat tissue caused the development of systemic insulin resistance and an increase in NF-κB activity in hepatic tissue; however, APC treatment suppressed leptin, insulin resistance, and NF-κB with its anti-inflammatory effect [10]. In the lipopolysaccharide-induced chronic cystitis model in mice, increased NF-κB-mediated inflammation has been shown to cause fibrosis and loss of function in the bladder [26]. In our study, an increase in NOX-2 – and NF-κB-immunopositive cells and histopathological tissue injury were found in the kidney and bladder in parallel with the high serum leptin level. APC treatment resulted in a decrease in serum leptin, tissue NOX-2, and NF-κB activity, as well as an improvement in histological findings. It has been stated that hyperfiltration is seen due to podocyte damage and volume increase in obesity [1], as well as inflammation of insulin resistance and activation of renin-angiotensin-aldosterone [5]. The specific staining of NF-κB in the macula densa, which is responsible for blood pressure and electrolyte regulation, was remarkable. However, the limitation of this study is that no correlation with renal function tests could be established. MPO, a neutrophil-derived enzyme, initiates the acute inflammatory response and has a role in the propagation of chronic inflammation through the ROS formation of such as NOX [12]. It has been reported that HFD feeding is associated with neutrophil and macrophage infiltration in the epididymal white adipose tissue and an increase in proinflammatory cytokines with the MPO enzyme, whereas these effects were not observed in MPO knockout mice [27]. APC has been shown to inhibit the translocation of p47phox, a subunit of NOX-2 activated by ROS and MPO, in endothelial and various leukocyte cells [12]. HFD has been shown to cause high oxidative damage, nitric oxide levels, infiltration of inflammatory cells, and activation of mast cells in the heart of obese rats, leading to a degeneration of myofibrils of the cardiac muscle [2]. Additionally, it was shown that HFD led to oxidative damage, an increase of IL-6, and tumor necrosis factor-α (TNF-α) levels with histopathological damage

http://doi.org/10.5472/marumj.1706664
Marmara Med J 2025;38(2): 171-178

in both kidney and bladder in rats [21]. In a model of ketamine-induced interstitial cystitis, severe mast cell infiltration has been shown to be associated with TGF-β signaling, an inflammatory and profibrotic cytokine, resulting in fibrosis and apoptosis [28]. In the current study, the number of mast cells in the bladder, inflammatory cell infiltration, histopathological tissue damage score, and MPO level increased in both the kidney and bladder in the HFD and HFD+DMSO groups in comparison with the control group. However, we observed that APC treatment decreased MPO levels in both the renal and bladder samples and the number of mast cells in the bladder thus repairing the histopathological damage.

Fibrosis is a prognostic factor for CKD [4]. TGF-β1 is the main factor of tissue scarring and has been shown to induce the transformation of fibroblasts into myofibroblasts [29]. Pathological collagen deposition can be demonstrated by picrosirius red staining that selectively stains type 1 and type 3 collagen [30]. Studies in obesity have shown that NOX-2-mediated ROS production damages the urinary system by activating inflammatory and profibrotic pathways such as NF-κB, IL-6, and TGF-β1 [4, 26]. Free fatty acids induce fibrosis, impair bladder muscle contraction [3, 6], and increase collagen between bladder muscle bundles in HFD-induced obesity [17]. Fayed et al., have shown that APC treatment ameliorates NOX-induced liver fibrosis by reducing α-smooth muscle actin (α-SMA) and TGF-β [11]. We showed that increased interstitial and glomerular collagen, increased TGF-β1 immunopositivity in kidney tissues, and increased collagen in the muscle layer of bladder tissue were observed in the HFD groups. These collagen deposits and TGF-β1 immunopositivity decreased in the HFD+APC compared with the HFD groups.

In conclusion, our results showed that HFD increased oxidative stress, inflammation, and fibrosis as well as decreased endogenous antioxidant levels and histopathological damage in both renal and bladder samples. Additionally, a NOX-2 inhibitor APC alleviates HFD-induced renal and bladder injury via inhibiting oxidative stress, inflammation, and fibrosis.

Acknowledgements

The authors would like to thank Dr. Dilek Akakın for comments on our manuscript.

Compliance with Ethical Standards

Ethical Approval: Ethcial approval for this study was obtained from Marmara University, School of Medicine Animal Care and Use Ethical Committee for Experimental Animals (date: 10.02.2022, approval no: 09.2020.mar).

Conflict of Interest: The authors declare that there are no conflicts of interest.

Financial Support: This study was financially supported by the Marmara University Scientific Research Project Committee (TTU: 2020-10107).

Author Contributions: FKM, GS, and FE: Contributed to the conception and design, FKM, BE, GS and FE: Performed experiments and did data collection, FKM, BE, GS and FE analyzed data. FKM and FE contributed to the writing of the article. All authors approved the final version of the article.

REFERENCES

[1] Bin-Meferij MM, El-Kott AF, Shati AA, Eid RA. Ginger extract ameliorates renal damage in high fat diet-ınduced obesity in rats: Biochemical and ultrastructural study. Int J Morphol 2019; 37: 438-47. doi: 10.4067/S0717.950.2201900.020.0438.

[2] Acikel-Elmas M, Cakıcı SE, Dur IR, et al. Protective effects of exercise on heart and aorta in high-fat diet-induced obese rats. Tissue Cell 2019; 57: 57-65. doi: 10.1016/j.tice.2019.01.005.

[3] Adedeji TG, Fasanmade AA, Olapade-Olaopa EO. Dietary macronutrients modulate hypertrophy and contractility of the detrusor in an experimental model of bladder obstruction. Pathophysiology 2019; 26: 11-20. doi: 10.1016/j.pathophys.2018.12.003.

[4] Avestaei AH, Yaghchiyan M, Ali-Hemmati A, Farhangi MA, Mesgari-Abbasi M, Shahabi P. Histological, metabolic, and inflammatory changes in the renal tissues of high-fat diet-induced obese rats after vitamin D supplementation. Nutr Food Sci 2020; 50: 1135-49. doi: 10.1108/NFS-01-2020-0009.

[5] Lakkis JI, Weir MR. Obesity and kidney disease. Prog Cardiovasc Dis 2018; 61: 157-67. doi: 10.1016/j.pcad.2018.07.005.

[6] Powers SA, Ryan TE, Pak ES, Fraser MO, McClung JM, Hannan JL. A chronic high-fat diet decreased detrusor mitochondrial respiration and increased nerve-mediated contractions. Neurourol Urodyn 2019; 38: 1524-32. doi: 10.1002/nau.24015.

[7] Alhasson F, Seth RK, Sarkar S, et al. High circulatory leptin-mediated NOX-2-peroxynitrite-miR21 axis activates mesangial cells and promotes renal inflammatory pathology in nonalcoholic fatty liver disease. Redox Biol 2018; 17: 1-15. doi: 10.1016/j.redox.2018.04.002.

[8] Bedard K, Krause KH. The NOX family of ROS-generating NADPH oxidases: physiology and pathophysiology. Physiol Rev 2007; 87: 245-313. doi: 10.1152/physrev.00044.2005.

[9] Suzuki S, Arnold LL, Pennington KL, Kakiuchi-Kiyota S, Cohen SM. Effects of coadministration of dietary sodium arsenite and an NADPH oxidase inhibitor on the rat bladder epithelium. Toxicology 2009; 261: 41-6. doi: 10.1016/j.tox.2009.04.042.

[10] Meng R, Zhu DL, Bi Y, Yang DH, Wang YP. Apocynin improves insulin resistance through suppressing inflammation in high-fat diet-induced obese mice. Mediators Inflamm 2010; 2010:858735. doi: 10.1155/2010/858735.

[11] Fayed MR, El-Naga RN, Akool ES, El-Demerdash E. The potential antifibrotic impact of apocynin and alpha-lipoic acid in concanavalin A-induced liver fibrosis in rats: Role of NADPH oxidases 1 and 4. Drug Discov Ther 2018; 12: 58-67. doi: 10.5582/ddt.2017.01065.

[12] Ximenes, VF, Kanegae, MP, Rissato, SR, Galhiane, MS. The oxidation of apocynin catalyzed by myeloperoxidase: Proposal for NADPH oxidase inhibition. Arch Biochem Biophys 2007; 457: 134-41. doi: 10.1016/j.abb.2006.11.010.

[13] Şener TE, Yüksel M, Özyılmaz-Yay N, et al. Apocynin attenuates testicular ischemia-reperfusion injury in rats. J Pediatr Surg 2015; 50: 1382-7. doi: 10.1016/j.jpedsurg.2014.11.033.

[14] Hersek İ, Köroğlu MK, Coşkunlu B, Ertaş B, Şener G, Ercan F. Apocynin ameliorates testicular toxicity in high-fat diet-fed rats by regulating oxidative stress. Clin Exp Health Sci 2023; 13: 75-83. doi: 10.33808/clinexphealthsci.1035133.

[15] Koyuncuoğlu T, Yıldırım A, Dertsiz EK, Yüksel M, Ercan F, Yeğen BÇ. Estrogen receptor agonists protect against acetaminophen-induced hepatorenal toxicity in rats. Life Sci 2020; 263: 118561. doi: 10.1016/j.lfs.2020.118561.

[16] Koca O, Gokce AM, Akyuz M, Ercan F, Yurdakul N, Karaman MI. A new problem in inflammatory bladder diseases: use of mobile phones! Braz J Urol 2014; 40: 520-5. doi: 10.1590/S1677-5538.IBJU.2014.04.11.

[17] de Souza AC, Gallo CBM, Passos MCDF, et al. Effect of a high-fat diet on the rat bladder wall and bioactive action of Brazil nut oil. Int Braz J Urol 2019; 45(1): 161-68. doi: 10.1590/S1677-5538.IBJU.2018.0547.

[18] Kanpalta Mustafaoglu F, Ertas B, Sen A, Akakin D, Sener G, Ercan F. *Myrtus communis* l. extract ameliorates high-fat diet-induced kidney and bladder damage by ınhibiting oxidative stress and ınflammation. Eur J Biol 2022; 81: 217-230. doi: 10.26650/EurJBiol.2022.111.1191.

[19] de Vries AP, Ruggenenti P, Ruan XZ, et al. Fatty kidney: emerging role of ectopic lipid in obesity-related renal disease. Lancet Diabetes Endocrinol 2014; 2: 417-26. doi: 10.1016/S2213-8587(14)70065-8.

[20] Kashiwagi E, Abe T, Kinoshita F, et al. The role of adipocytokines and their receptors in bladder cancer: expression of adiponectin or leptin is an independent prognosticator. Am J Transl Res 2020; 12: 3033-45.

[21] Acikel Elmas M, Ozakpınar OB, Kolgazi M, Sener G, Ercan F. Morphological and biochemical investigation of the healing effects of exercise on high-fat diet-induced kidney and bladder damage. Clin Exp Health Sci 2022; 12: 817-23. doi: 10.33808/clinexphealthsci.1027516.

[22] Acikel Elmas M, Ozgun G, Bingol Ozakpinar O, Guleken Z, Arbak S. Effects of apocynin against monosodium glutamate-ınduced oxidative damage in rat kidney. Eur J Biol 2022; 81: 231-39. doi: 10.26650/EurJBiol.2022.114.8934.

[23] Wu LL, Chiou CC, Chang PY, Wu JT. Urinary 8-OHdG: a marker of oxidative stress to DNA and a risk factor for cancer, atherosclerosis, and diabetics. Clin Chim Acta 2004; 339: 1-9. doi: 10.1016/j.cccn.2003.09.010.

[24] Lee M, Zhao H, Liu Xet al. Protective effect of hydroxysafflor yellow a on nephropathy by attenuating oxidative stress and inhibiting apoptosis in induced type 2 diabetes in rat. Oxid Med Cell Longev 2020; 7805393. doi: 10.1155/2020/7805393.

[25] Cheng SF, Jiang YH, Kuo HC. Urothelial dysfunction and chronic ınflammation are associated with increased bladder sensation in patients with chronic renal insufficiency. Int Neurourol J. 2018; 22 (Suppl 1): S46-54. doi: 10.5213/inj.1832814.407.

[26] Lai J, Ge M, Shen S, et al. Activation of NFKB-JMJD3 signaling promotes bladder fibrosis via boosting bladder smooth muscle cell proliferation and collagen accumulation. Biochim Biophys Acta Mol Basis Dis 2019; 1865: 2403-10. doi: 10.1016/j.bbadis.2019.05.008.

[27] Wang Q, Xie Z, Zhang W, et al. Myeloperoxidase deletion prevents high-fat diet-induced obesity and insulin resistance. Diabetes 2014; 63:4172-85. doi: 10.2337/db14-0026.

[28] Kim A, Yu HY, Heo J, et al. Mesenchymal stem cells protect against the tissue fibrosis of ketamine-induced cystitis in rat bladder. Sci Rep 2016; 6: 30881. doi: 10.1038/srep30881.

[29] Bondi CD, Manickam N, Lee DY, et al. NAD(P)H oxidase mediates TGF-beta1-induced activation of kidney myofibroblasts. J Am Soc Nephrol 2010; 21: 93-102. doi: 10.1681/ASN.200.902.0146.

[30] Junqueira LC, Bignolas G, Brentani RR. Picrosirius staining plus polarization microscopy, a specific method for collagen detection in tissue sections. Histochem J 1979; 11: 447-55. doi: 10.1007/BF01002772.